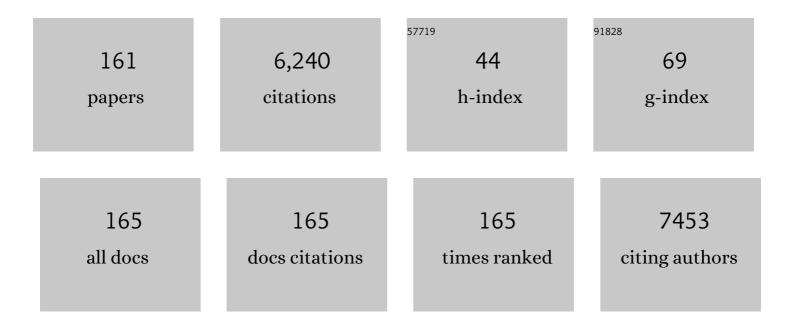
List of Publications by Year in descending order

Source: https://exaly.com/author-pdf/9295339/publications.pdf Version: 2024-02-01



#	Article	IF	CITATIONS
1	Polysulfide Speciation and Migration in Catholyte Lithiumâ^'Sulfur Cells. ChemPhysChem, 2022, 23, .	1.0	4
2	Electro hemoâ€Mechanical Modeling of Artificial Solid Electrolyte Interphase to Enable Uniform Electrodeposition of Lithium Metal Anodes. Advanced Energy Materials, 2022, 12, .	10.2	105
3	Visualization of Dissolutionâ€Precipitation Processes in Lithium–Sulfur Batteries. Advanced Energy Materials, 2022, 12, .	10.2	24
4	Accelerating Battery Characterization Using Neutron and Synchrotron Techniques: Toward a Multiâ€Modal and Multiâ€Scale Standardized Experimental Workflow. Advanced Energy Materials, 2022, 12, .	10.2	17
5	Electroâ€Chemoâ€Mechanical Modeling of Artificial Solid Electrolyte Interphase to Enable Uniform Electrodeposition of Lithium Metal Anodes (Adv. Energy Mater. 9/2022). Advanced Energy Materials, 2022, 12, .	10.2	1
6	Effect of the Niobium Doping Concentration on the Charge Storage Mechanism of Mesoporous Anatase Beads as an Anode for High-Rate Li-Ion Batteries. ACS Applied Energy Materials, 2021, 4, 215-225.	2.5	13
7	Insight into the Critical Role of Exchange Current Density on Electrodeposition Behavior of Lithium Metal. Advanced Science, 2021, 8, 2003301.	5.6	146
8	Structure and dynamics of highly concentrated LiTFSI/acetonitrile electrolytes. Physical Chemistry Chemical Physics, 2021, 23, 13819-13826.	1.3	14
9	Pressure and Temperature Dependence of Local Structure and Dynamics in an Ionic Liquid. Journal of Physical Chemistry B, 2021, 125, 2719-2728.	1.2	16
10	Critical Role of Functional Groups Containing N, S, and O on Graphene Surface for Stable and Fast Charging Li‧ Batteries. Small, 2021, 17, e2007242.	5.2	23
11	Real-time imaging of Na ⁺ reversible intercalation in "Janus―graphene stacks for battery applications. Science Advances, 2021, 7, .	4.7	61
12	High-frequency dynamics and test of the shoving model for the glass-forming ionic liquid Pyr14-TFSI. Physical Review Materials, 2021, 5, .	0.9	2
13	Promoted rate and cycling capability of Li–S batteries enabled by targeted selection of co-solvent for the electrolyte. Energy Storage Materials, 2020, 25, 131-136.	9.5	23
14	A flexible and free-standing FeS/sulfurized polyacrylonitrile hybrid anode material for high-rate sodium-ion storage. Chemical Engineering Journal, 2020, 385, 123453.	6.6	54
15	Designing Highly Conductive Functional Groups Improving Guest–Host Interactions in Li/S Batteries. Small, 2020, 16, e1905585.	5.2	28
16	Stable lithium metal anode enabled by high-dimensional lithium deposition through a functional organic substrate. Energy Storage Materials, 2020, 33, 158-163.	9.5	19
17	Role of Liâ€lon Depletion on Electrode Surface: Underlying Mechanism for Electrodeposition Behavior of Lithium Metal Anode. Advanced Energy Materials, 2020, 10, 2002390.	10.2	115
18	Enhancement of Functional Properties of Liquid Electrolytes for Lithiumâ€Ion Batteries by Addition of Pyrrolidiniumâ€Based Ionic Liquids with Long Alkyl hains. Batteries and Supercaps, 2020, 3, 1059-1068.	2.4	7

#	Article	IF	CITATIONS
19	Fast charging negative electrodes based on anatase titanium dioxide beads for highly stable Li-ion capacitors. Materials Today Energy, 2020, 16, 100424.	2.5	11
20	Density scaling of structure and dynamics of an ionic liquid. Physical Chemistry Chemical Physics, 2020, 22, 14169-14176.	1.3	15
21	Recent Developments and Future Challenges in Designing Rechargeable Potassium-Sulfur and Potassium-Selenium Batteries. Energies, 2020, 13, 2791.	1.6	13
22	Electrochemical Behaviour of Nbâ€Đoped Anatase TiO ₂ Microbeads in an Ionic Liquid Electrolyte. Batteries and Supercaps, 2020, 3, 1233-1238.	2.4	10
23	Amine―and Amideâ€Functionalized Mesoporous Carbons: A Strategy for Improving Sulfur/Host Interactions in Li–S Batteries. Batteries and Supercaps, 2020, 3, 757-765.	2.4	10
24	Design of a Multifunctional Interlayer for NASCIONâ€Based Solidâ€ S tate Li Metal Batteries. Advanced Functional Materials, 2020, 30, 2001444.	7.8	109
25	Charge storage mechanism of α-MnO2 in protic and aprotic ionic liquid electrolytes. Journal of Power Sources, 2020, 460, 228111.	4.0	16
26	Stable Li metal anode by crystallographically oriented plating through in-situ surface doping. Science China Materials, 2020, 63, 1036-1045.	3.5	15
27	A VO2 based hybrid super-capacitor utilizing a highly concentrated aqueous electrolyte for increased potential window and capacity. Electrochimica Acta, 2020, 345, 136225.	2.6	12
28	Highly Stable Fe ₃ O ₄ /C Composite: A Candidate Material for All Solid-State Lithium-Ion Batteries. Journal of the Electrochemical Society, 2020, 167, 070556.	1.3	10
29	Designing a Safe Electrolyte Enabling Long‣ife Li/S Batteries. ChemSusChem, 2019, 12, 4176-4184.	3.6	26
30	Boosting High Energy Density Lithium-Ion Storage via the Rational Design of an FeS-Incorporated Sulfurized Polyacrylonitrile Fiber Hybrid Cathode. ACS Applied Materials & Interfaces, 2019, 11, 29924-29933.	4.0	44
31	Comparison of ionic liquid electrolyte to aqueous electrolytes on carbon nanofibres supercapacitor electrode derived from oxygen-functionalized graphene. Chemical Engineering Journal, 2019, 375, 121906.	6.6	45
32	Enhanced safety and galvanostatic performance of high voltage lithium batteries by using ionic liquids. Electrochimica Acta, 2019, 316, 1-7.	2.6	32
33	Enhanced ionic conductivity and interface stability of hybrid solid-state polymer electrolyte for rechargeable lithium metal batteries. Energy Storage Materials, 2019, 23, 105-111.	9.5	102
34	Stable ionic-liquid-based symmetric supercapacitors from Capsicum seed-porous carbons. Journal of Electroanalytical Chemistry, 2019, 838, 119-128.	1.9	42
35	A free-standing reduced graphene oxide aerogel as supporting electrode in a fluorine-free Li2S8 catholyte Li-S battery. Journal of Power Sources, 2019, 416, 111-117.	4.0	45
36	V ₂ O ₅ Cryogel: A Versatile Electrode for All Solid State Lithium Batteries. Journal of the Electrochemical Society, 2019, 166, A3927-A3931.	1.3	2

#	Article	IF	CITATIONS
37	Melt-Mixed 3D Hierarchical Graphene/Polypropylene Nanocomposites with Low Electrical Percolation Threshold. Nanomaterials, 2019, 9, 1766.	1.9	23
38	Low Dose X-Ray Speckle Visibility Spectroscopy Reveals Nanoscale Dynamics in Radiation Sensitive Ionic Liquids. Physical Review Letters, 2018, 120, 168001.	2.9	28
39	An Electrospun Nanofiber Membrane as Gelâ€Based Electrolyte for Roomâ€Temperature Sodium–Sulfur Batteries. Energy Technology, 2018, 6, 1214-1219.	1.8	19
40	Byproduct-free curing of a highly insulating polyethylene copolymer blend: an alternative to peroxide crosslinking. Journal of Materials Chemistry C, 2018, 6, 11292-11302.	2.7	26
41	Free-Standing 3D-Sponged Nanofiber Electrodes for Ultrahigh-Rate Energy-Storage Devices. ACS Applied Materials & Interfaces, 2018, 10, 34140-34146.	4.0	18
42	Minimizing the Electrolyte Volume in Li–S Batteries: A Step Forward to High Gravimetric Energy Density. Advanced Energy Materials, 2018, 8, 1801560.	10.2	68
43	An Electrospun Core–Shell Nanofiber Web as a Highâ€Performance Cathode for Iron Disulfideâ€Based Rechargeable Lithium Batteries. ChemSusChem, 2018, 11, 3625-3630.	3.6	13
44	Rational Design of Low Cost and High Energy Lithium Batteries through Tailored Fluorineâ€ f ree Electrolyte and Nanostructured S/C Composite. ChemSusChem, 2018, 11, 2981-2986.	3.6	20
45	Tailor-Made Electrospun Multilayer Composite Polymer Electrolytes for High-Performance Lithium Polymer Batteries. Journal of Nanoscience and Nanotechnology, 2018, 18, 6499-6505.	0.9	9
46	A high-power and fast charging Li-ion battery with outstanding cycle-life. Scientific Reports, 2017, 7, 1104.	1.6	37
47	A mixed mechanochemical-ceramic solid-state synthesis as simple and cost effective route to high-performance LiNi0.5Mn1.5O4 spinels Electrochimica Acta, 2017, 235, 262-269.	2.6	16
48	Achieving enhanced ionic mobility in nanoporous silica by controlled surface interactions. Physical Chemistry Chemical Physics, 2017, 19, 5727-5736.	1.3	34
49	Stabilizing the Performance of High apacity Sulfur Composite Electrodes by a New Gel Polymer Electrolyte Configuration. ChemSusChem, 2017, 10, 3490-3496.	3.6	20
50	Route to sustainable lithium-sulfur batteries with high practical capacity through a fluorine free polysulfide catholyte and self-standing Carbon Nanofiber membranes. Scientific Reports, 2017, 7, 6327.	1.6	18
51	Corrigendum to "Electropolished Titanium Implants with a Mirror-Like Surface Support Osseointegration and Bone Remodelling― Advances in Materials Science and Engineering, 2017, 2017, 1-2.	1.0	0
52	Electropolished Titanium Implants with a Mirror-Like Surface Support Osseointegration and Bone Remodelling. Advances in Materials Science and Engineering, 2016, 2016, 1-10.	1.0	4
53	A binder-free sulfur/reduced graphene oxide aerogel as high performance electrode materials for lithium sulfur batteries. Scientific Reports, 2016, 6, 39615.	1.6	38
54	Long-term osseointegration of 3D printed CoCr constructs with an interconnected open-pore architecture prepared by electron beam melting. Acta Biomaterialia, 2016, 36, 296-309.	4.1	120

#	Article	IF	CITATIONS
55	Sulfur-doped ordered mesoporous carbons: A stability-improving sulfur host for lithium-sulfur battery cathodes. Journal of Power Sources, 2016, 317, 112-119.	4.0	47
56	lonic liquid and hybrid ionic liquid/organic electrolytes for high temperature lithium-ion battery application. Electrochimica Acta, 2016, 216, 24-34.	2.6	64
57	Aggregation behavior of aqueous cellulose nanocrystals: the effect of inorganic salts. Cellulose, 2016, 23, 3653-3663.	2.4	115
58	Enhanced low-temperature ionic conductivity via different Li ⁺ solvated clusters in organic solvent/ionic liquid mixed electrolytes. Physical Chemistry Chemical Physics, 2016, 18, 25458-25464.	1.3	35
59	Formation and relaxation kinetics of starch–particle complexes. Soft Matter, 2016, 12, 9509-9519.	1.2	18
60	The Orientation of Nanoscale Apatite Platelets in Relation to Osteoblastic–Osteocyte Lacunae on Trabecular Bone Surface. Calcified Tissue International, 2016, 98, 193-205.	1.5	32
61	3D printed Ti6Al4V implant surface promotes bone maturation and retains a higher density of less aged osteocytes at the bone-implant interface. Acta Biomaterialia, 2016, 30, 357-367.	4.1	163
62	Competitive adsorption of amylopectin and amylose on cationic nanoparticles: a study on the aggregation mechanism. Soft Matter, 2016, 12, 3388-3397.	1.2	13
63	Structural Origin of the Mixed Glass Former Effect in Sodium Borophosphate Glasses Investigated with Neutron Diffraction and Reverse Monte Carlo Modeling. Journal of Physical Chemistry C, 2015, 119, 27275-27284.	1.5	12
64	Effect of Water on the Local Structure and Phase Behavior of Imidazolium-Based Protic Ionic Liquids. Journal of Physical Chemistry B, 2015, 119, 1611-1622.	1.2	59
65	Polysulfide-containing Glyme-based Electrolytes for Lithium Sulfur Battery. Chemistry of Materials, 2015, 27, 4604-4611.	3.2	105
66	Alkali-ion concentration dependence of the structure of proton-conducting alkali thio-hydroxogermanates investigated with neutron diffraction. Solid State Ionics, 2015, 274, 40-45.	1.3	1
67	The effect of lithium salt doping on the nanostructure of ionic liquids. Physical Chemistry Chemical Physics, 2015, 17, 27082-27087.	1.3	38
68	A structural study of LiTFSI–tetraglyme mixtures: From diluted solutions to solvated ionic liquids. Journal of Molecular Liquids, 2015, 210, 238-242.	2.3	62
69	Role of organic solvent addition to ionic liquid electrolytes for lithium–sulphur batteries. RSC Advances, 2015, 5, 2122-2128.	1.7	21
70	Coordination and interactions in a Li-salt doped ionic liquid. Journal of Non-Crystalline Solids, 2015, 407, 318-323.	1.5	46
71	Liquid 1-propanol studied by neutron scattering, near-infrared, and dielectric spectroscopy. Journal of Chemical Physics, 2014, 140, 124501.	1.2	68
72	Electrochemical properties of a full cell of lithium iron phosphate cathode using thin amorphous silicon anode. Solid State Ionics, 2014, 268, 256-260.	1.3	15

#	Article	IF	CITATIONS
73	Analysis of the solid electrolyte interphase formed with an ionic liquid electrolyte for lithium-sulfur batteries. Journal of Power Sources, 2014, 252, 150-155.	4.0	109
74	Structure and properties of Li-ion conducting polymer gel electrolytes based on ionic liquids of the pyrrolidinium cation and the bis(trifluoromethanesulfonyl)imide anion. Journal of Power Sources, 2014, 245, 830-835.	4.0	45
75	In-situ gelled electrolyte for lithium battery: Electrochemical andÂRaman characterization. Journal of Power Sources, 2014, 245, 232-235.	4.0	8
76	Road maps of no use to some physicists. Nature, 2014, 507, 169-169.	13.7	1
77	Electrochemical characterization of poly(vinylidene fluoride-co-hexafluoro propylene) based electrospun gel polymer electrolytes incorporating room temperature ionic liquids as green electrolytes for lithium batteries. Solid State Ionics, 2014, 262, 77-82.	1.3	23
78	Effect of carbon coating methods on structural characteristics and electrochemical properties of carbon-coated lithium iron phosphate. Solid State Ionics, 2014, 262, 25-29.	1.3	11
79	Characterization of N-butyl-N-methyl-pyrrolidinium bis(trifluoromethanesulfonyl)imide-based polymer electrolytes for high safety lithium batteries. Journal of Power Sources, 2013, 224, 93-98.	4.0	73
80	Silica/alkali ratio dependence of the microscopic structure of sodium silicate solutions. Journal of Colloid and Interface Science, 2013, 397, 9-17.	5.0	28
81	Nano-fibrous polymer films for organic rechargeable batteries. Journal of Materials Chemistry A, 2013, 1, 2426-2430.	5.2	45
82	The temperature dependent structure of liquid 1-propanol as studied by neutron diffraction and EPSR simulations. Journal of Chemical Physics, 2013, 138, 214501.	1.2	42
83	Lithium Ion Conducting Boron-Oxynitride Amorphous Thin Films: Synthesis and Molecular Structure by Infrared Spectroscopy and Density Functional Theory Modeling. Journal of Physical Chemistry C, 2013, 117, 7202-7213.	1.5	13
84	Physical Properties, Ion–Ion Interactions, and Conformational States of Ionic Liquids with Alkyl-Phosphonate Anions. Journal of Physical Chemistry B, 2013, 117, 8172-8179.	1.2	26
85	Ionic liquids for energy applications. MRS Bulletin, 2013, 38, 533-537.	1.7	70
86	A New Class of Ionic Liquids: Anion Amphiprotic Ionic Liquids. Journal of Physical Chemistry Letters, 2012, 3, 2114-2119.	2.1	13
87	Preparation and application of TEMPO-based di-radical organic electrode with ionic liquid-based polymer electrolyte. RSC Advances, 2012, 2, 10394.	1.7	14
88	2,3,6,7,10,11-Hexamethoxytriphenylene (HMTP): A new organic cathode material for lithium batteries. Electrochemistry Communications, 2012, 21, 50-53.	2.3	12
89	Polymer electrolytes based on poly(vinylidene fluoride-co-hexafluoropropylene) nanofibrous membranes containing polymer plasticizers for lithium batteries. Solid State Ionics, 2012, 225, 631-635.	1.3	27
90	1H NMR study of the hydrogen dynamics in the (NaS)xGe(OH)4â^'x·yH2O ceramic proton conductors. Solid State Ionics, 2012, 228, 46-55.	1.3	1

#	Article	IF	CITATIONS
91	Electrochemical properties of lithium polymer batteries with doped polyaniline as cathode material. Materials Research Bulletin, 2012, 47, 2815-2818.	2.7	23
92	Improving the stability of an organic battery with an ionic liquid-based polymer electrolyte. RSC Advances, 2012, 2, 9795.	1.7	23
93	Effect of Lithium Salt on the Stability of Dispersions of Fumed Silica in the Ionic Liquid BMImBF ₄ . Langmuir, 2012, 28, 4080-4085.	1.6	50
94	A statistical model of hydrogen bond networks in liquid alcohols. Journal of Chemical Physics, 2012, 136, 094514.	1.2	49
95	Phase behaviour, transport properties, and interactions in Li-salt doped ionic liquids. Faraday Discussions, 2012, 154, 71-80.	1.6	77
96	Towards flexible secondary lithium batteries: polypyrrole-LiFePO4 thin electrodes with polymer electrolytes. Journal of Materials Chemistry, 2012, 22, 15045.	6.7	44
97	Selective growth of double-walled carbon nanotubes on gold films. Materials Letters, 2012, 72, 78-80.	1.3	19
98	Templated Growth of Covalently Bonded Threeâ€Dimensional Carbon Nanotube Networks Originated from Graphene. Advanced Materials, 2012, 24, 1576-1581.	11.1	37
99	Ionic liquids and oligomer electrolytes based on the B(CN)4â^' anion; ion association, physical and electrochemical properties. Physical Chemistry Chemical Physics, 2011, 13, 14953.	1.3	29
100	Highly porous LiMnPO4 in combination with an ionic liquid-based polymer gel electrolyte for lithium batteries. Electrochemistry Communications, 2011, 13, 1105-1108.	2.3	43
101	Conformational evolution of TFSI ^{â^`} in protic and aprotic ionic liquids. Journal of Raman Spectroscopy, 2011, 42, 522-528.	1.2	119
102	Concentration- and pH-dependence of highly alkaline sodium silicate solutions. Journal of Colloid and Interface Science, 2011, 356, 37-45.	5.0	52
103	Properties of N-butyl-N-methyl-pyrrolidinium Bis(trifluoromethanesulfonyl) Imide Based Electrolytes as a Function of Lithium Bis(trifluoromethanesulfonyl) Imide Doping. Journal of the Korean Electrochemical Society, 2011, 14, 92-97.	0.1	15
104	Short-range structure of proton-conducting BaM0.10Zr0.90O2.95 (M=Y, In, Sc and Ga) investigated with vibrational spectroscopy. Solid State Ionics, 2010, 181, 126-129.	1.3	38
105	Synthesis and characterization of a lactic acidâ€based thermoset resin suitable for structural composites and coatings. Journal of Applied Polymer Science, 2010, 115, 480-486.	1.3	37
106	The conductivity of pyrrolidinium and sulfonylimide-based ionic liquids: A combined experimental and computational study. Journal of Power Sources, 2010, 195, 2074-2076.	4.0	52
107	An imidazolium based ionic liquid electrolyte for lithium batteries. Journal of Power Sources, 2010, 195, 7639-7643.	4.0	146
108	Using Neutron Spinâ^'Echo To Investigate Proton Dynamics in Proton-Conducting Perovskites. Chemistry of Materials, 2010, 22, 740-742.	3.2	43

7

#	Article	IF	CITATIONS
109	Temperature-Dependent Infrared Spectroscopy of Proton-Conducting Hydrated Perovskite Baln _{<i>x</i>} Zr _{1â^'<i>x</i>} Zr _{1â^'<i>x</i>} O _{3â^'<i>x</i>/2} (<i>x</i> C). Journal of Physical Chemistry C, 2010, 114, 6177-6181.	1.5	13
110	Aggregation, ageing and transport properties of surface modified fumed silica dispersions. Soft Matter, 2010, 6, 2293.	1.2	41
111	Quasielastic neutron scattering of hydrated BaZr0.90A0.10O2.95 (A=Y and Sc). Solid State Ionics, 2009, 180, 22-28.	1.3	36
112	Phase Behavior and Ionic Conductivity in Lithium Bis(trifluoromethanesulfonyl)imide-Doped Ionic Liquids of the Pyrrolidinium Cation and Bis(trifluoromethanesulfonyl)imide Anion. Journal of Physical Chemistry B, 2009, 113, 11247-11251.	1.2	107
113	Thermal Properties and Ionic Conductivity of Imidazolium Bis(trifluoromethanesulfonyl)imide Dicationic Ionic Liquids. Journal of Physical Chemistry B, 2009, 113, 10607-10610.	1.2	85
114	Effect of functionalized silica particles on cross-linked poly(vinyl alcohol) proton conducting membranes. Journal of Applied Electrochemistry, 2008, 38, 931-938.	1.5	16
115	Crystal Structure and Proton Conductivity of BaZr _{0.9} Sc _{0.1} O _{3â^´î´} . Journal of the American Ceramic Society, 2008, 91, 3039-3044.	1.9	43
116	Location of deuteron sites in the proton conducting perovskite BaZr0.50In0.50O3â^'y. Journal of Alloys and Compounds, 2008, 450, 103-110.	2.8	62
117	Short-Range Structure of Proton-Conducting Perovskite Baln _{<i>x</i>} Zr _{1-<i>x</i>} O _{3-<i>x</i>/2} (<i>x</i> = 0a^0.75). Chemistry of Materials, 2008, 20, 3480-3486.	3.2	75
118	Structure of Proton-Conducting Alkali Thio-Hydroxogermanates. Chemistry of Materials, 2008, 20, 6014-6021.	3.2	7
119	mathvariant="normal">O <mml:mtext>å^`</mml:mtext> <mml:mi mathvariant="normal">Hwag vibrations in hydrated<mml:math xmlns:mml="http://www.w3.org/1998/Math/MathML" display="inline"><mml:mrow><mml:msub><mml:mi>Baln</mml:mi><mml:mi< td=""><td>1.1</td><td>27</td></mml:mi<></mml:msub></mml:mrow></mml:math </mml:mi 	1.1	27
120	mathvariant="bold-italic">x <mml:msub><mml:msub><mml:mi>Zr</mml:mi><mml:mrow><mml:mn Proton Conduction in Perovskite Oxide BaZr[sub 0.5]Yb[sub 0.5]O[sub 3â^1] Prepared by Wet Chemical Synthesis Route. Journal of the Electrochemical Society, 2008, 155, P97.</mml:mn </mml:mrow></mml:msub></mml:msub>	1.3	16
121	Structure of glassy lithium sulfate films sputtered in nitrogen: Insight from Raman spectroscopy and <i>ab initio</i> calculations. Physical Review B, 2008, 77, .	1.1	8
122	Comment on "Glass-Specific Behavior in the Damping of Acousticlike Vibrations― Physical Review Letters, 2007, 98, 079601; author reply 079602.	2.9	16
123	MaticetÂal.Reply:. Physical Review Letters, 2007, 98, .	2.9	1
124	A Structural Study on Ionic-Liquid-Based Polymer Electrolyte Membranes. Journal of the Electrochemical Society, 2007, 154, G183.	1.3	38
125	Physical Properties of Proton Conducting Membranes Based on a Protic Ionic Liquid. Journal of Physical Chemistry B, 2007, 111, 12462-12467.	1.2	99
126	Neutron diffraction and far-infrared spectroscopy of proton conducting alkali thio-hydroxogermanates. Solid State Ionics, 2007, 178, 501-505.	1.3	4

#	Article	IF	CITATIONS
127	A study on the state of PWA in PVDF-based proton conducting membranes by Raman spectroscopy. Solid State Ionics, 2007, 178, 527-531.	1.3	15
128	Structural study and proton conductivity in Yb-doped BaZrO3. Solid State Ionics, 2007, 178, 515-520.	1.3	59
129	New evidence of light-induced structural changes detected in As–S glasses by photon energy dependent Raman spectroscopy. Journal of Non-Crystalline Solids, 2006, 352, 1607-1611.	1.5	20
130	The Debye–Waller factor approaching the glass-transition temperature in phosphate glasses. Journal of Non-Crystalline Solids, 2006, 352, 4577-4582.	1.5	1
131	Concentration effects on irreversible colloid cluster aggregation and gelation of silica dispersions. Journal of Colloid and Interface Science, 2006, 301, 137-144.	5.0	21
132	Structural analysis of PVA-based proton conducting membranes. Solid State Ionics, 2006, 177, 2431-2435.	1.3	60
133	Temperature dependent infrared spectroscopy of proton conducting alkali thio-hydroxogermanates. Solid State Ionics, 2006, 177, 1009-1013.	1.3	6
134	Proton conductivity and low temperature structure of In-doped BaZrO3. Solid State Ionics, 2006, 177, 2357-2362.	1.3	60
135	Synthesis and structural characterization of perovskite type proton conducting BaZr1â^'xInxO3â^'δ (0.0â‰æâ‰ 0 .75). Solid State Ionics, 2006, 177, 1395-1403.	1.3	65
136	Structure and functionality of PVdF/PAN based, composite proton conducting membranes. Electrochimica Acta, 2005, 50, 3992-3997.	2.6	23
137	Vibrational properties of proton conducting double perovskites. Solid State Ionics, 2005, 176, 2971-2974.	1.3	28
138	Vibrational properties of protons in hydratedBaInxZr1â^'xO3â^'xâ^•2. Physical Review B, 2005, 72, .	1.1	71
139	Dynamics around the sol-gel transition in thermoreversible atactic polystyrene gels. AIP Conference Proceedings, 2004, , .	0.3	Ο
140	Accelerating effects of colloidal nano-silica for beneficial calcium–silicate–hydrate formation in cement. Chemical Physics Letters, 2004, 392, 242-248.	1.2	530
141	Frequency dependent conductivity of single alkali and mixed alkali phosphate glasses. Journal of Non-Crystalline Solids, 2004, 345-346, 514-517.	1.5	1
142	Crystal-Like Nature of Acoustic Excitations in Glassy Ethanol. Physical Review Letters, 2004, 93, 145502.	2.9	32
143	Signatures of a drying SiO2·(H2O)x gel from Raman spectroscopy and quantum chemistry. Chemical Physics Letters, 2003, 380, 165-172.	1.2	31
144	Ionic conductivity and the mixed alkali effect inLixRb1â^'xPO3glasses. Physical Review B, 2003, 68, .	1.1	32

#	Article	IF	CITATIONS
145	High-frequency collective excitations in a molecular glass-former. Journal of Physics Condensed Matter, 2003, 15, S1259-S1267.	0.7	3
146	Acoustic modes in the network glass Li2O-2B2O3: New evidence from inelastic X-ray scattering. The Philosophical Magazine: Physics of Condensed Matter B, Statistical Mechanics, Electronic, Optical and Magnetic Properties, 2002, 82, 243-249.	0.6	0
147	Dynamics of silver phosphate glasses by light and neutron scattering measurements. The Philosophical Magazine: Physics of Condensed Matter B, Statistical Mechanics, Electronic, Optical and Magnetic Properties, 2002, 82, 257-262.	0.6	0
148	Dielectric modulus analysis of mixed alkali LixRb1â~'xPO3 glasses. Journal of Non-Crystalline Solids, 2002, 307-310, 1012-1016.	1.5	21
149	Dynamics of silver phosphate glasses by light and neutron scattering measurements. The Philosophical Magazine: Physics of Condensed Matter B, Statistical Mechanics, Electronic, Optical and Magnetic Properties, 2002, 82, 257-262.	0.6	2
150	Contrasting behaviour of acoustic modes in network and non-network glasses. Europhysics Letters, 2001, 54, 77-83.	0.7	47
151	Random ion distribution model: A structural approach to the mixed-alkali effect in glasses. Physical Review B, 2001, 63, .	1.1	99
152	Sound Wave Scattering in Network Glasses. Physical Review Letters, 2001, 86, 3803-3806.	2.9	51
153	Experimental insight into the mixed mobile ion effect in glasses. Solid State Ionics, 2000, 136-137, 1055-1060.	1.3	9
154	Free volume and dissociation effects in fast ion conducting glasses. Journal of Non-Crystalline Solids, 2000, 263-264, 73-81.	1.5	7
155	Conductivity enhancement inPbI2â^'AgIâ^'AgPO3glasses by diffraction experiments and reverse Monte Carlo modeling. Physical Review B, 1999, 60, 12023-12032.	1.1	27
156	lonic motion of silver in super-ionic glasses. Physica B: Condensed Matter, 1999, 266, 69-74.	1.3	10
157	Structure of mixed alkali phosphate glasses by neutron diffraction and Raman spectroscopy. Physical Review B, 1998, 58, 11331-11337.	1.1	60
158	Structure and dynamics of phosphate glasses. The Philosophical Magazine: Physics of Condensed Matter B, Statistical Mechanics, Electronic, Optical and Magnetic Properties, 1998, 77, 357-362.	0.6	25
159	Changes in the structure of AgI-AgPO3 around the glass transition temperature. Solid State Ionics, 1996, 86-88, 421-424.	1.3	10
160	Influence of Zn-doping on the electronic raman scattering of YBa2Cu3O7 â~ δ. Journal of Physics and Chemistry of Solids, 1995, 56, 1835.	1.9	3
161	Structural Study and Conductivity of BaZr0.90Ga0.10O2.95. Ceramic Engineering and Science Proceedings, 0, , 105-117.	0.1	1